



HAL
open science

MAGIX, a new software for the analysis of complex gamma spectra

Isabelle Espagnon, P.G. Allinei, Anne-Catherine Simon, M. Delarue, Yves Pontillon

► **To cite this version:**

Isabelle Espagnon, P.G. Allinei, Anne-Catherine Simon, M. Delarue, Yves Pontillon. MAGIX, a new software for the analysis of complex gamma spectra. *Applied Radiation and Isotopes*, 2023, 191, pp.110505. 10.1016/j.apradiso.2022.110505 . cea-03963171

HAL Id: cea-03963171

<https://cea.hal.science/cea-03963171>

Submitted on 30 Jan 2023

HAL is a multi-disciplinary open access archive for the deposit and dissemination of scientific research documents, whether they are published or not. The documents may come from teaching and research institutions in France or abroad, or from public or private research centers.

L'archive ouverte pluridisciplinaire **HAL**, est destinée au dépôt et à la diffusion de documents scientifiques de niveau recherche, publiés ou non, émanant des établissements d'enseignement et de recherche français ou étrangers, des laboratoires publics ou privés.

MAGIX, a new software for the analysis of complex gamma spectra

I. Espagnon^a, P. G. Alline^b, A. C. Simon^a, M. Delarue^b, and Yves Pontillon^c

^aUniversité Paris-Saclay, CEA, List, F-91120, Palaiseau France

^bCEA, DES, IRESNE, DTN, SMTA, Nuclear Measurement Laboratory, Cadarache, F-13108 Saint-Paul-Lez-Durance, France

^cCEA, DES, IRESNE, DEC, SA3E, LAMIR, Cadarache, F-13108 Saint-Paul-Lez-Durance, France

Abstract

The MAGIX code (a French acronym standing for Automatic Gamma and X-ray Measurement) is a software developed to analyze γ/X spectra on the topic of severe accident diagnosis. Indeed, the gamma spectra obtained after a severe reactor core accident are complex because they are composed of hundreds of lines of short-lived fission products and Fukushima accident demonstrated a lack in robustness of data interpretation during a crisis. MAGIX allows a complete and entirely automatic analysis of the spectra, with identification of radionuclides and calculation of activities. It can analyze spectra measured by detectors with excellent resolution such as HPGe detectors as well as detectors with medium resolution (e.g. CZT and LaBr₃). For most detectors, the analysis of the spectra can be done without a detection efficiency curve because its process can include the calculation of a relative detection efficiency. MAGIX accepts spectra corresponding to any experimental setup (energy slope, energy range, resolution, absorber, etc.). However, these experimental conditions can have an impact on the quality of the results. Results on spectra simulated in different configurations showed that the analysis of the HPGe spectrum with the user defined efficiency and with the MAGIX detection efficiency were close. Furthermore, they also showed that the accuracy of activities was similar with increasing energy slopes but decreased with resolution degradation, with fewer correctly identified radionuclides in this case.

Keywords

Activities, DECA-PF project, fission products, gamma spectrometry, MAGIX code, spectral analysis

1. Introduction

Many spectra analysis software exist and give satisfactory results when detection efficiency is known and the number of lines is not too large [1]-[2]. In the field of severe nuclear accident, the gamma spectra of fission products show hundreds of peaks with many risks of errors such as interferences or unresolved peaks. In this case, the development of a gamma ray library is a complex operation, which requires strong expertise and enough time to select the correct gamma ray emissions. These last two constraints are rarely met in a crisis context. In the last few years, new software based on convolutional neural network trained with synthetic spectra has appeared [3] but this approach requires a radionuclide list and a fixed experimental setup, which is incompatible with an accident context.

The MAGIX code was developed as part of the DECA-PF project (Diagnosis of a degraded reactor core through

Fission Product measurements) [4]. The aim of DECA-PF project is to improve the evaluation of radioactive releases into the environment, and to provide a diagnostic tool for the state of the core in support of crisis teams, based on the measurement of the emitted Fission Products (FPs). This project led to an instrumentation partly based on measuring stations equipped with low resolution gamma spectrometers imposed by the need to carry out measurements in post-accident situations. Another part of the project was to develop specific code to automatically analyze these spectra.

MAGIX was designed from the expertise acquired with the development of two previous gamma spectrometry codes: the IGA code that determines the isotopic composition of plutonium and uranium [5] from HPGe spectra and the sIGAle code that determines activities of radionuclides using CZT detector with asymmetric peaks [6].

The principle of MAGIX is based on the automatic analysis of the γ/X spectrum emitted by the different radionuclides and measured with High Purity Germanium (HPGe), Cadmium Zinc Telluride (CZT), or Lanthanum Bromide (LaBr₃) detectors. MAGIX is able to analyze spectra corresponding to any experimental setup (gain, energy range, resolution, absorber, etc.), without any detailed data on the setup being necessary and without detection efficiency curve for spectra with Full Width at Half Maximum (FWHM) lower than 3 % at 662 keV. The user can control all intermediate results with an Internet browser interface.

The first part of this paper presents the general principles of spectrum processing and a detailed description of each part of the code. Then, results on simulated spectra corresponding to different detectors and experimental setups will be given and discussed. Finally, an example of use of MAGIX on measured photofission spectra will be provided.

2. Description of MAGIX code

2.1. General presentation of the processing

The aim of the spectrum analysis is to identify radionuclides present in the spectrum and to calculate the activity of each radionuclide if detection efficiency is known, or to estimate activity ratios if detection efficiency is unknown. Each peak in the spectrum is linked to the different radionuclides by its position (that gives qualitative information) and its net area (that gives quantitative information). Fig. 1 shows the MAGIX general algorithm for the processing of a spectrum measured with an HPGe detector or with a room temperature spectrometer (CZT, LaBr₃) with a FWHM lower than 3% at 662 keV. After a rough energy and resolution calibration, the analysis begins with a preliminary stage of radionuclide identification: the radionuclides present in the spectrum are identified in order to select the radionuclides that MAGIX will use in the following step. Then, the fine calibration step is highly important, involving energy self-calibration and spectrum shape. If the detection efficiency is unknown, the next stage, which is carried out twice, consists in calculating the relative detection efficiency. The last stage, which is also carried out twice, is the estimation of the activities or of the activity ratios. Consistency tests complete the analysis. As shown in Fig. 1, two stages have common modules: the filtering of the nuclear and atomic database and the analysis (or deconvolution) of the regions.

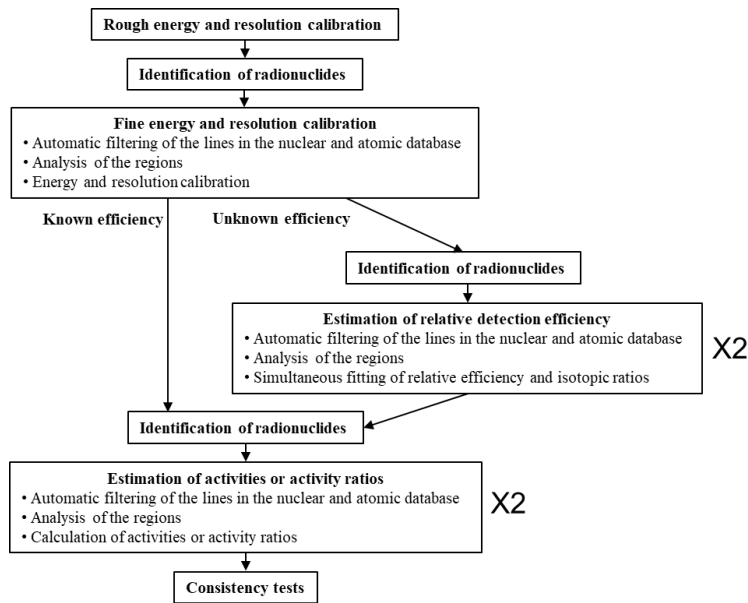


Fig. 1: MAGIX general algorithm for high-resolution spectrum.

In case of high-count rate or electronic degradation of the signal, room temperature detectors produce spectra with FWHM greater than 3% at 662 keV. Thus, the algorithm has to be “simplified” because several stages are difficult or even impossible to perform: the fine energy and resolution calibration and the estimation of detection efficiency. Fig. 2 shows the general algorithm for low-resolution spectrum.

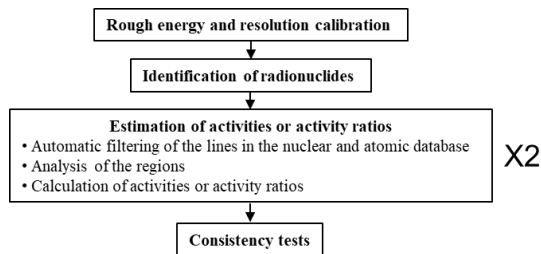


Fig. 2: MAGIX general algorithm for low-resolution spectrum.

2.2. User input data

The code requires, in addition to the spectrum in counts, very little mandatory input data from the user to carry out the processing: two channel-energy pairs chosen by the user and the FWHM relative to a user-selected energy. The user can add optional data such as the detection efficiency curve to facilitate the analysis or a pair of values (energy, absolute detection efficiency) to calculate activities.

2.3. Atomic and nuclear database

The general atomic and nuclear database of MAGIX contains 1339 radionuclides (52000 lines) with all the necessary information relative to the energy, the intensity and the natural width of all the X-ray [5] and gamma lines [7] of the radionuclides sought by the code. By default, MAGIX uses a reduced database of 190 radionuclides. If necessary, the users can easily modify this radionuclide list to create their own reduced

database. A line selection will be then automatically performed by MAGIX throughout the spectrum processing (§ 2.5).

2.4. Identification of radionuclides

The identification of radionuclides begins with a peak search in the spectrum (Fig. 3). The peak search module used is based on a classical property of the second derivative of the spectrum, which is to be negative under the peaks. This stage leads to a list of peak energies in the spectrum. Then, an association of these found peaks is done with the lines contained in the atomic and nuclear database. The lines are considered as candidates if their energies are sufficiently close to the energy of the found peaks. A presence probability is computed for each radionuclide from the intensities of the candidate lines weighted by the detection efficiency curve.

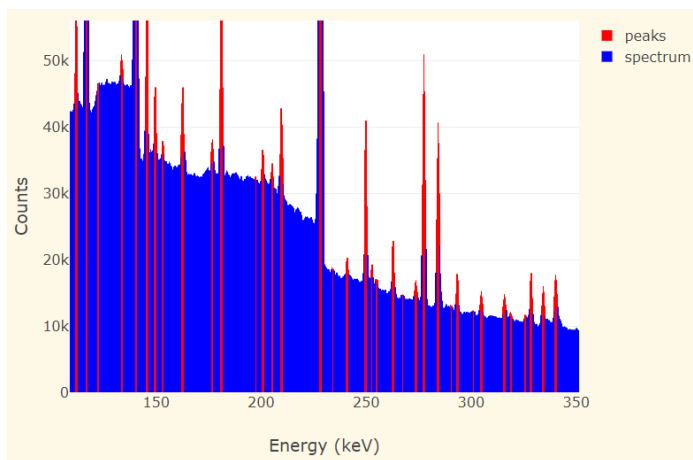


Fig. 3: Example of peaks found in a HPGe spectrum.

Some radionuclides, even if not found by the radionuclides identification step, can be added if they belong to certain decay chains and if at least one radionuclide in the chain has been found. Indeed, some elements are not always easily detectable, but taking them into account is nevertheless essential for the deconvolution of the regions of interest.

The radionuclide identification stage is carried out several times throughout the spectrum processing. It will be more reliable after the fine calibration sequence.

2.5. Atomic and nuclear database filtering

At the beginning of each stage (fine calibration, determination of the relative detection efficiency and calculation of activities), the database is automatically filtered to retain only the lines considered a priori to be the most pertinent, and grouped in regions of interest. To do so, a succession of filters is applied, such as:

- elimination of the lines of the radionuclides not selected by the radionuclide identification module, as described above,
- elimination of the lines with low weighted intensity in absolute terms,
- elimination of the lines of low weighted intensity relative to other lines of the same energy.

Finally, the remaining lines are grouped in regions, separated by distances depending on the spectrum resolution. If these regions are too large (in the case of many lines with a low resolution for example), the regions are split again according to the spectrum. Moreover, in the case of the fine calibration step, the regions containing more

than two distinct energy lines are deleted to avoid disturbing the self-calibration by analyzing complex regions at a stage when little is known about the spectrum.

Thus, the automatic database filtering depends on each spectrum and each step.

2.6. Region analysis

The purpose of the region analysis module is to adjust the content of the channels in each of the regions of interest selected by the database filter module, in order to determine the variables needed in the current module (heights, positions and standard deviations for fine calibration, heights for the other stages). The content of the channels is fitted by a model that takes into account both a background and the peaks corresponding to the lines selected for the region. Each peak is modelled by a Gaussian and the background is modelled with a unique polynomial function on the entire region. The complete fitting of the region is carried out by a sequential quadratic programming method, enabling numerous variables and constraints to be taken into consideration. The latter include constraints between peak heights, when they relate to the same radionuclide. Two examples of deconvolved regions are given in Fig. 4 (high-resolution spectrum) and in Fig. 5 (low-resolution spectrum). In low-resolution spectra, the regions are generally larger and more complex to fit.

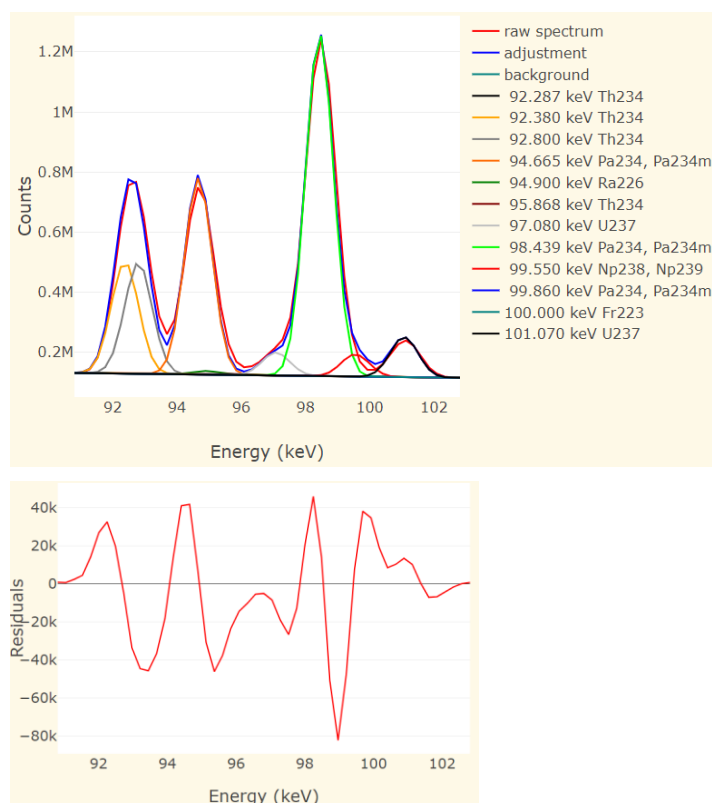


Fig. 4: Example of deconvolved region between 91 and 103 keV and residuals of the fit for a measured high-resolution spectrum (HPGe).

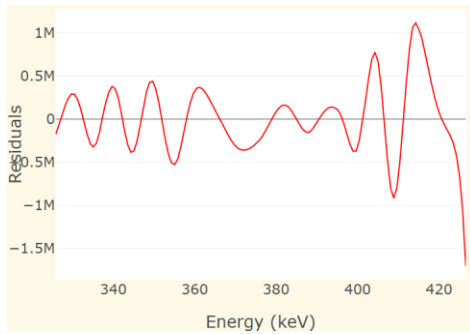
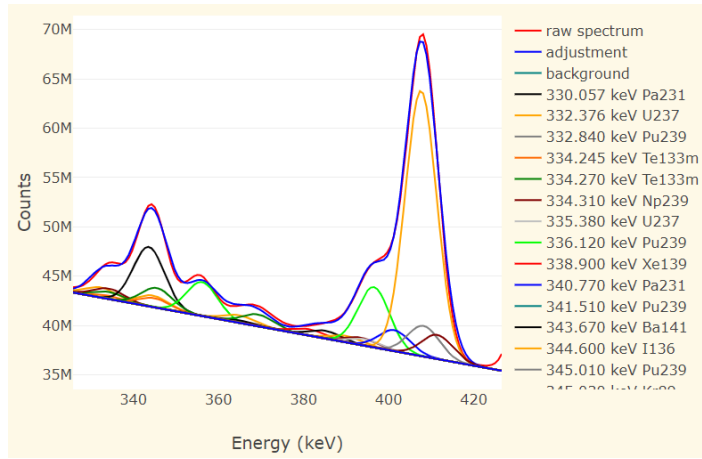


Fig. 5: Example of deconvolved region between 320 and 430 keV and residuals of the fit for a simulated low-resolution spectrum.

A first selection is then done on the fitted peaks according to criteria on detection limit and fit quality.

In some cases, corrections of the fitted areas can be made for radionuclides containing only mixed lines (a line is called mixed when it is associated with several radionuclides) and for the main line of radionuclides that may be confused, during deconvolution, with other lines close in energy.

2.7. Determination of relative detection efficiency

In case of high-resolution spectrum, if the absolute detection efficiency curve has not been provided by the user, a relative detection efficiency is calculated by MAGIX as follows:

The relative detection efficiency curve can be written in two different ways:

- the first one is given by the net areas measured in the spectrum thanks to the deconvolution of regions and the mass fractions sought:

$$\varepsilon(E) = \frac{S(E)}{\sum_{i=1}^{n_{iso}} \frac{f_i I_i(E_i)}{T_i A_i}}$$

where:

- $S(E)$ is the measured net area of a peak at energy E ,
- f_i is the mass fraction of radionuclide i relative to a reference radionuclide,
- $I_i(E_i)$ is the probability of photon emission of radionuclide i at energy E_i ,
- T_i and A_i are the period in seconds and the atomic mass of radionuclide i ,

- the second one is given by an energy-dependent parametric model; this parametric model uses three terms:

$$\varepsilon(P, E) = \varepsilon_{att}(E)\varepsilon_{self-att}(E)\varepsilon_{detector}(E)$$

with:

- ε_{att} the attenuation in an absorber:

$$\varepsilon_{att}(E) = \exp(-\mu_{absorber}(E) \cdot x_{absorber})$$

- $\varepsilon_{self-att}$ the self-attenuation in a matrix:

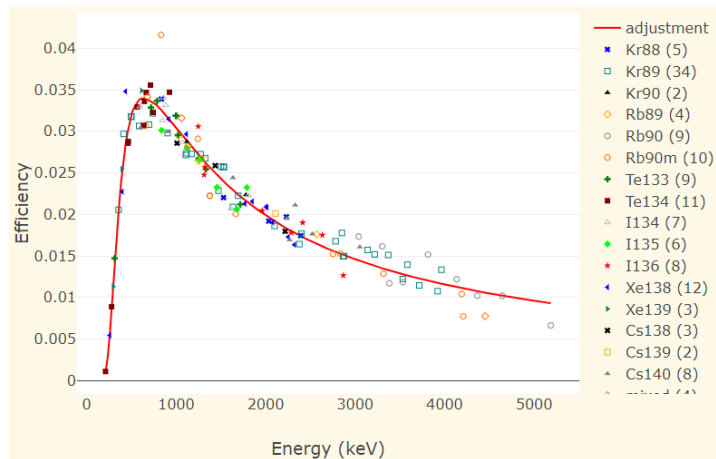
$$\varepsilon_{self-att}(E) = \frac{1 - \exp(-\mu_{matrix}(E) \cdot x_{matrix})}{\mu_{matrix}(E) \cdot x_{matrix}}$$

- $\varepsilon_{detector}$ an analytical expression representing the detection efficiency of the detector:

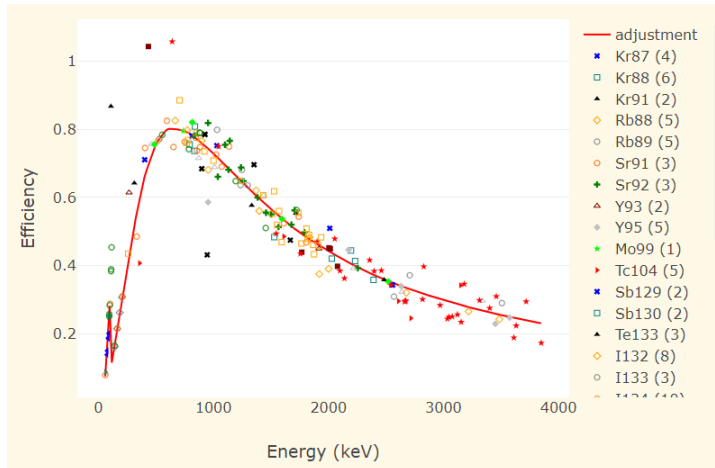
$$\varepsilon_{detector}(E) = \frac{\exp(a_1)E^{a_2}}{\left(1 + \left(\frac{E}{a_3}\right)^3\right)^{a_4}}$$

μ is the linear attenuation coefficient and x the thickness. The set of parameters P of the function $\varepsilon(P, E)$ are the parameters of the 3 components, namely unknown $x_{absorber}$, x_{matrix} , a_1 , a_2 , a_3 and a_4 . If there are any, the user can indicate to MAGIX the presence of absorbers (Pb, Cd, ...) or matrix (U, Pu). Par default, MAGIX uses a cadmium absorber.

The difference between both types of description of $\varepsilon(E)$ is then globally minimized on all the selected peaks, by a weighted adjustment of the unknown parameters (mass fractions and detection efficiency parameters). In this optimization, one of the mass fractions remains fixed and thus serves as a reference for all the other mass fractions, as well as for the resulting relative detection efficiency curve. Fig. 6, for instance, shows two relative detection efficiency curves obtained by this type of analysis.



(a)



(b)

Fig. 6: Example of a relative detection efficiency curves obtained after optimization. In these examples, the efficiency contains 2 terms. (a): the detector efficiency and the attenuation in a lead absorber. (b): the detector efficiency and the self-attenuation in uranium (depleted uranium sample). The presence of a lead absorber or an U matrix has been indicated by the user.

The detection efficiency calculated by MAGIX is a relative efficiency. If the user provides a pair of values (energy, absolute detection efficiency), MAGIX can compute the absolute detection efficiency:

$$\epsilon_{absolute}(E) = \epsilon_{MAGIX}(E) \frac{\epsilon_{user}(E_{user})}{\epsilon_{MAGIX}(E_{user})}$$

where:

- $\epsilon_{MAGIX}(E)$ is the relative detection efficiency computed by MAGIX at energy E ,
- E_{user} and $\epsilon_{user}(E_{user})$ are the energy and the absolute detection efficiency provided by the user.

2.8. Study of the consistency between the lines of the radionuclide

For each radionuclide, MAGIX studies the consistency between its lines by comparing the fitted areas to the expected areas. The expected areas are calculated for each line energy from the fitted area of the line with the largest theoretical area:

$$S_{expected}(E) = \frac{fI(E)}{TA} \epsilon(E) \frac{S_{fitted}(E_1)}{S_{theoretical}(E_1)}$$

where:

- f is the mass fraction of the radionuclide,
- $I(E)$ is the probability of photon emission of the radionuclide at energy E ,
- T and A are the period in seconds and the atomic mass of the radionuclide,
- $\epsilon(E)$ is the detection efficiency at energy E ,
- E_1 is the energy corresponding to the largest theoretical area and:

$$S_{theoretical}(E_1) = \frac{fI(E_1)}{AT} \epsilon(E_1)$$

For each line, MAGIX calculates the R ratio between the expected area and the fitted area. Only lines above limit of detection are taken into account. The expected areas are then divided by the median of R values so as to give preference to the greatest number of coherent lines between them. The R ratio is recalculated from these

new expected areas. Only peaks with an R value between 0.5 and 2 are selected. An example is presented in Table 1 with the ^{87}Kr lines. In the table, the lines are sorted by decreasing expected areas. The R values are between 0.4 and 1.11. There is a good consistency between the lines when the R values are close to 1. In this example, the second line is not coherent with the others ($R = 0.4$) and will be removed for the following sequence. The fitted area of the 845 keV line is larger than the expected value because when fitting the region, there was a confusion between the 845.44 keV line of ^{87}Kr and the 844.36 keV line of ^{133}Te : all the ^{133}Te counts were wrongly attributed to ^{87}Kr .

Table 1: Example of R values for ^{87}Kr lines.

Energy (keV)	Fitted areas	Expected areas	R = Expected / Fitted areas
402.59	1398	1558	1.11
845.44	755	300	0.40
2554.8	226	226	1.00
2558.1	96	96	1.00

The peaks are sorted by decreasing expected areas.
Green = selected line, orange = removed line ($R < 0.5$ or $R > 2$).

2.9. Radionuclide selection

To be selected, a radionuclide has to meet several conditions, such as:

- at least one of the two main lines must be selected,
- if less than one third of the lines are selected (above the limit of detection), the sum of the expected areas must be greater than 50%.

A consistency test is also performed between the smoothed spectrum (a smoothing of the initial spectrum is performed with a Savitzky-Golay filter in order to minimize statistical fluctuations) and the reconstructed spectrum (a synthetic spectrum is reconstructed from the detection efficiency and the mass fractions (cf. §2.11)). For each radionuclide, MAGIX calculates the χ^2 between the smoothed spectrum and the reconstructed spectrum at the energies around the lines of the radionuclide. If the χ^2 value is too large, the radionuclide is not selected.

2.10. Activities and activity ratios

Once the list of selected radionuclides has been established and the expected areas calculated, MAGIX can calculate either the activities if absolute detection efficiency is known or the activity ratios if it is not.

2.10.1. Activities

The activity of each radionuclide is calculated from the expected areas (all the lines provide the same activity):

$$Act = \frac{S_{expected}(E)}{t \cdot I(E) \cdot \varepsilon_{absolute}(E)}$$

where:

- Act is the calculated activity, in Becquerels,
- $S_{expected}(E)$ is the expected area of the peak at the energy E , in counts,
- t is the acquisition time, in seconds,
- $I(E)$ is the probability of photon emission at energy E (without unit),
- $\varepsilon_{absolute}(E)$ is the absolute detection efficiency at energy E (without unit).

For each line of the radionuclide, an activity uncertainty is calculated. It takes into account the uncertainty on the fitted area ($\sigma_S(E)=\sqrt{S}$) and the uncertainty on the detection efficiency ($\sigma_\varepsilon(E)$):

$$\frac{\sigma_{Act}(E)}{Act(E)} = \sqrt{\left(\frac{\sigma_S(E)}{S(E)}\right)^2 + \left(\frac{\sigma_\varepsilon(E)}{\varepsilon(E)}\right)^2}$$

In “known efficiency” mode, σ_ε can be provided by the user together with the absolute detection efficiency curve. In “unknown efficiency” mode, σ_ε is calculated from the dispersion of points around the relative detection efficiency curve. The true coincidence summing (TCS) corrections are not applied in this analysis because in the configurations envisaged for the use of MAGIX, the TCS effects are small or negligible.

The uncertainty on the activity of the radionuclide is calculated differently depending on whether the radionuclide contains one or more lines:

- if the radionuclide has only one line, the uncertainty of the radionuclide is the uncertainty of the line,
- if the radionuclide contains several lines, MAGIX takes the largest uncertainty between the uncertainty of the main line and the standard deviation of the activities calculated from the fitted areas, weighted by the expected areas.

2.10.2. Activity ratios

If the absolute detection efficiency is unknown, MAGIX cannot calculate activities but activity ratios.

As activity of a radionuclide i can be written using its mass:

$$Act_i = \lambda_i N_i = \frac{\ln 2}{T_i} \cdot \frac{N_A m_i}{A_i}$$

where:

- λ_i is the decay constant of radionuclide i ,
- N_i is the number of atoms of radionuclide i ,
- N_A is the Avogadro number,
- m_i is the mass of radionuclide i ,
- T_i and A_i are the period in seconds and the atomic mass of radionuclide i .

The activity ratio between two radionuclides is:

$$Act_{12} = \frac{Act_1}{Act_2} = \frac{m_1}{m_2} \cdot \frac{A_2}{A_1} \cdot \frac{T_2}{T_1}$$

where m_1/m_2 is the mass ratio, determined at the same time as the relative detection efficiency.

Activity ratios are normalized and presented in %.

2.10.3. Confidence degree

For each radionuclide, its activity (or its activity ratio) is provided with its uncertainty and, in some cases, with warnings.

Eight warnings can accompany the result, such as:

- the main line is missing,
- only one line is selected,

- the sum of the selected area is lower than 50% of the sum of the expected areas.

These warnings help the user to assign a degree of confidence: the higher the number of warnings, the more carefully the result should be taken. The meanings for the warnings can help the user to validate or not the presence of the radionuclide.

2.11. Consistency analysis

At the end of the analysis, two types of consistency tests are carried out on the results:

- In the first test, a synthetic spectrum is reconstructed from the mass fraction results, the detection efficiency and the Gaussian peak model, and compared graphically with the original spectrum. In order to have comparable backgrounds on both spectra, one background is calculated by the orthogonal polynomial method [8] on each zone of the original spectrum, then added to the synthetic spectrum (Fig. 7).

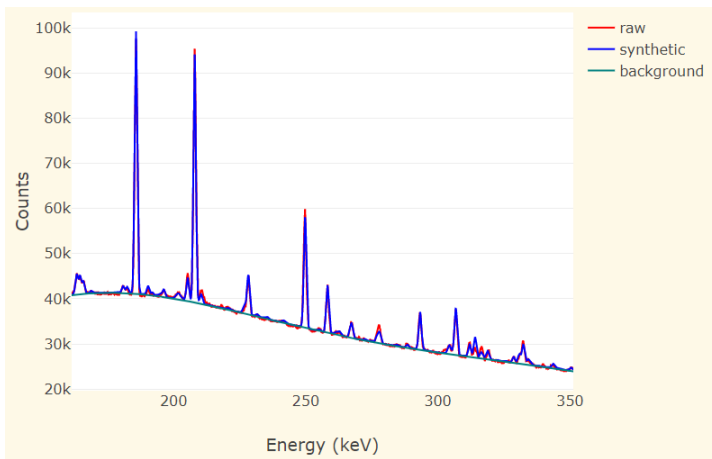


Fig. 7: Comparison of raw and synthetic spectra (700 keV - 900 keV region).

- The second test consists in searching for peaks present in the original spectrum and absent in the synthetic spectrum (called unreconstructed peaks). The goal is to verify that MAGIX has not forgotten any radionuclides in its analysis. If unreconstructed peaks are found, MAGIX searches for possible candidate radionuclides. To do this, the energies of these unreconstructed peaks are compared to the energies of the first two major lines of all the radionuclides in the complete atomic and nuclear database (1339 radionuclides). The lines are selected if their energy is sufficiently close to the energy of the unreconstructed peak.

Table 2 presents an example of unreconstructed peak found by MAGIX. MAGIX proposes several candidates, including ^{51}Cr . In this case, the missing radionuclide is ^{51}Cr (simulated spectrum), which is not present in the reduced database used by default by MAGIX.

Table 2: Example of unreconstructed peak with candidate radionuclides.

Energy (keV)	Areas	LD	Candidates for major line (ΔE in keV)	Candidates for second line (ΔE in keV)
320.14	4210	750	^{51}Cr (0.06) ^{51}Ti (0.06)	^{119}I (-0.39) ^{107}In (-0.80)

LD (Limit of Detection) $9 \cdot \sqrt{FWHM \cdot B}$ with $FWHM$ in keV and B the background noise in counts per keV [9]. In addition to the degree of confidence in the results given by the software itself, these types of tests allow the user to verify these results.

3. Results and discussion

The purpose of this part is to assess MAGIX performance. This work was carried out from simulated spectra with different resolutions and energy slopes. A first use of MAGIX has also been performed using real spectra.

3.1. Simulated spectra

We simulated spectra with the MCNP code [10], which allowed us to know precisely the initial activities of the different radionuclides. After the MCNP spectrum simulation for a 1 cm^3 cubic CZT, the "pulse height tally" was convoluted with the real peak shapes experimentally obtained with calibration sources. Three spectrometers were simulated from real detectors tested in the laboratory: 30% coaxial HPGe [11], 1 cm^3 CZT [12] and 1.5×1.5 LaBr₃ [13].

The simulations shown in Fig. 8 correspond to gamma spectra acquired by HPGe, CZT, and LaBr₃ detectors on gas species fission products accumulated on a trapping media. The energies of the spectra range from 0 to 2.5 MeV. Table 3 presents the resolutions and the energy slopes of the spectra. They contain 36 radionuclides above the limit of detection. The main radionuclides are ^{132}Te , ^{131}I , ^{132}I and ^{133}I .

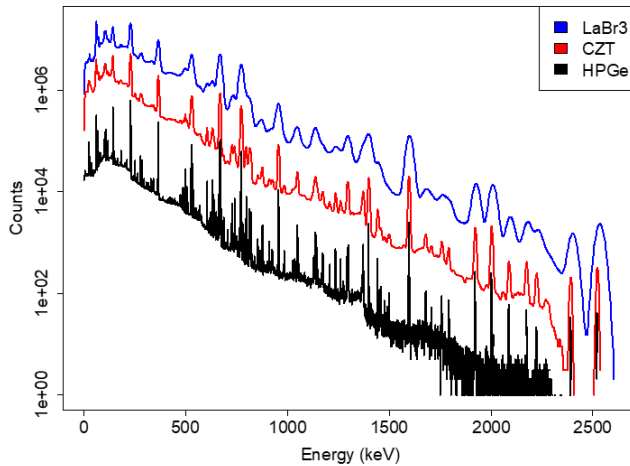


Fig. 8: Simulated spectra with several resolutions (HPGe, CZT and LaBr₃ spectra).

Table 3: Energy slopes and resolutions of HPGe, CZT and LaBr₃ spectra.

Detector	Energy slope (keV/channel)	FWHM at 662 keV (%)
HPGe	0.32	0.2
CZT	0.95	1.2
LaBr ₃	0.95	3.2

3.2. Estimation of the detection efficiency

The spectra were analyzed by MAGIX with and without the user defined efficiency (which is a simulated detection efficiency here). In the unknown efficiency mode, MAGIX calculated a relative detection efficiency curve that was normalized to absolute detection efficiency with a pair of values (energy, absolute detection efficiency) given by the user. Fig. 9 shows the user defined efficiency and the normalized relative detection efficiencies calculated by MAGIX for HPGe and CZT spectra. The detection efficiency estimated by MAGIX from the HPGe spectrum was very close to the user defined efficiency. The MAGIX detection efficiency estimated from the CZT spectrum was slightly further from the user defined efficiency and was defined over a lower energy range.

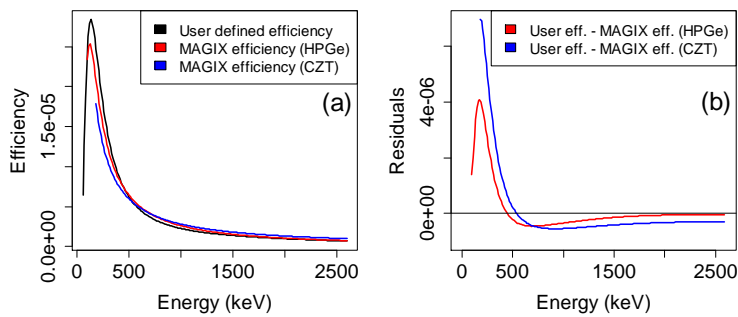


Fig. 9: (a): User defined efficiency and MAGIX detection efficiencies obtained from HPGe and CZT spectra. (b): Residuals between user defined efficiency and MAGIX efficiency.

3.3. Activities

The aim of the analysis was to identify the radionuclides present in the spectrum and to calculate ratio of activities or activities when detection efficiency was known. The analysis of the HPGe, CZT and LaBr₃ spectra showed that more radionuclides were found with the HPGe spectrum than with CZT and LaBr₃ spectra (Fig. 10). With the user defined efficiency (in known efficiency mode), 32 radionuclides were correctly found with the HPGe spectrum compared to 18 and 17 with CZT and LaBr₃ spectra. With the MAGIX detection efficiency (in unknown efficiency mode), the result was similar: 32 with the HPGe spectrum and 17 with the CZT spectrum. The median value of the ratio of the reference activity to MAGIX activity was around 1 for the three spectra but it was a little better with the user defined efficiency: 1.01 (HPGe) and 1.05 (CZT and LaBr₃) with the user defined efficiency against 1.08 (HPGe) and 1.13 (CZT) with the MAGIX detection efficiency. In the same way, the interquartile range was a little lower with the user defined efficiency than with the MAGIX detection efficiency and was lower with the HPGe spectrum than with CZT and LaBr₃ spectra.

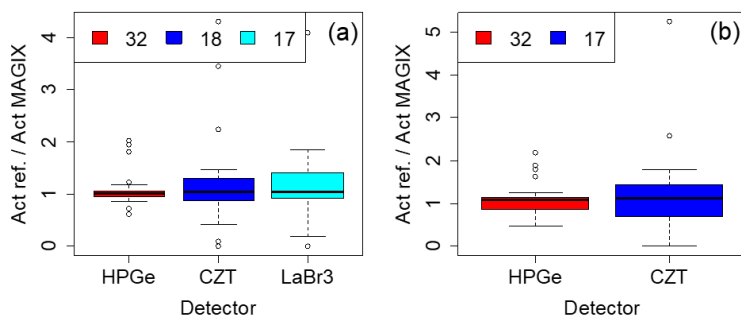


Fig. 10: The ratios of reference activity to MAGIX activity obtained for HPGe, CZT and LaBr₃ spectra (a): with user defined efficiency (b): with MAGIX detection efficiency. The numbers in the legend indicate the number of found radionuclides.

An example of MAGIX results is given in Table 4 with the activities calculated by MAGIX from the HPGe spectrum with the user defined efficiency. For each found radionuclide, MAGIX provided its activity with its uncertainty and a confidence index (number of warnings). In Table 4, the radionuclides are sorted by increasing number of warnings, with a color code by number of warnings. A large number of warnings was usually associated with a low activity. Nevertheless, it was not always the case. For example, the ^{99m}Tc radionuclide had a high activity (well calculated) with 2 warnings: its activity was calculated from a single line (= 1 warning) that was mixed (= 1 warning).

MAGIX always provides the causes of the warnings to help the user to interpret the results.

Table 4: MAGIX results for HPGe spectrum with user defined efficiency.

Radio-nuclide	MAGIX/ MDA	MAGIX (Bq)	Uncertainty (%)	Warning number	Ref/ MAGIX
^{132}Te	943.4	1.69e+07	11	.	1.1
^{132}I	850.6	1.84e+07	7	.	1
^{131}I	661.6	1.77e+07	8	.	0.9
^{133}I	348.8	1.09e+07	3	.	1
^{239}Np	135.2	1.01e+07	6	.	0.9
^{103}Ru	94.0	2.72e+06	1	.	1
^{134}Cs	80.4	2.05e+06	11	.	1
^{99}Mo	36.9	1.09e+07	9	.	1
^{140}La	29.0	1.71e+06	9	.	1
^{136}Cs	18.7	9.01e+05	11	.	1
^{140}Ba	14.4	3.69e+06	5	.	1
^{135}I	11.8	6.63e+05	8	.	1
^{131m}Te	11.5	1.7e+06	37	.	0.6
^{127}Sb	10.0	1.12e+06	12	.	1.1
^{95}Zr	3.4	1.27e+05	15	.	0.9
^{91}Sr	3.4	2.95e+05	51	.	0.7
^{110m}Ag	2.2	5.07e+04	4	.	1.1
^{137m}Ba	60.8	1.51e+06	1	1	1
^{95}Nb	59.4	1.17e+06	1	1	1
^{135}Xe	43.3	8.62e+05	4	1	1
^{141}Ce	36.4	1.22e+06	5	1	1
^{215}Bi	6.7	5.55e+05	2	1	.
^{143}Ce	6.1	2.8e+05	2	1	2
^{144}Ce	5.5	8.26e+05	5	1	1
^{91m}Y	3.7	1.08e+05	2	1	1.1
^{92}Rb	3.0	1.68e+06	3	1	.
^{105}Rh	2.5	2.78e+05	3	1	1.2
^{129}Te	2.5	8.9e+05	3	1	0.9
^{96}Sr	2.4	5.25e+04	14	1	.
^{99m}Tc	466.3	8.43e+06	5	2	1
^{133}Xe	17.8	1.11e+06	7	2	0.9
^{131}Te	8.0	1.98e+05	3	2	1.2
^{125}Sb	1.9	1.64e+05	3	2	0.7
^{132}Sn	1.3	6.46e+04	9	2	.
^{238}Np	1.1	7.76e+04	6	2	1.8
^{212}Bi	1.9	6.04e+05	3	3	.
^{135m}Xe	1.6	5.25e+04	3	3	2
^{142}Cs	1.5	1.27e+05	2	3	.

MAGIX = activity calculated by MAGIX, Ref = reference activity,

MDA (Minimum Detectable Activity) = $\frac{LD}{t \cdot (\epsilon I)_{max}}$ with t the acquisition time and $(\epsilon I)_{max}$ the product of the absolute detection efficiency and the probability of photon emission at the energy where this product is maximum.

The radionuclides are sorted by increasing number of warnings.

Green = no warning, orange = 1 warning, purple = 2 warnings and red = more than 2 warnings.

In this example, 38 radionuclides were found by MAGIX:

- 32 radionuclides were really present in the simulated spectrum. Among them, 17 radionuclides were found without warnings, 9 with one warning and 6 with more than one warning (Fig. 11a). The ratios of reference activity to MAGIX activity varied between 0.6 (^{131m}Te) and 2 (^{143}Ce and ^{135m}Xe). Fig. 11b presents the relative differences between MAGIX activities and the reference activities with their uncertainties according to the reference activities and shows a good coherence between them.

- 6 radionuclides were not present in the spectrum but warnings were reported for these radionuclides (2 with 3 warnings, 1 with 2 warnings and 3 with 1 warning) and, for the majority, their activities were close to the minimum detectable activity (MDA). The activity of ^{215}Bi , which was found 6.7 times above the MDA, was calculated from a single line (293.56 keV) that was confused with the 293.266 keV line of ^{143}Ce , really present in the spectrum. The activity of ^{143}Ce , also calculated from a single line, is therefore underestimated (Ref / MAGIX = 2 because it lacks the ^{215}Bi counts).

- 4 simulated radionuclides were not found by MAGIX: ^{106}Rh (3.3MDA), ^{111}Ag (2.5MDA), ^{129m}Te (1.8MDA) and ^{97}Nb (1.1MDA). The first three radionuclides were not found by MAGIX in the radionuclide identification module (peaks corresponding to the main lines were not found) and ^{97}Nb was removed from the MAGIX analysis because there was a confusion between the 657.94 keV line of ^{97}Nb and the 657.76 keV mixed line of ^{110}Ag and ^{110m}Ag in the fitting of the region: all the ^{97}Nb counts were wrongly attributed to ^{110}Ag , ^{110m}Ag mixed line.

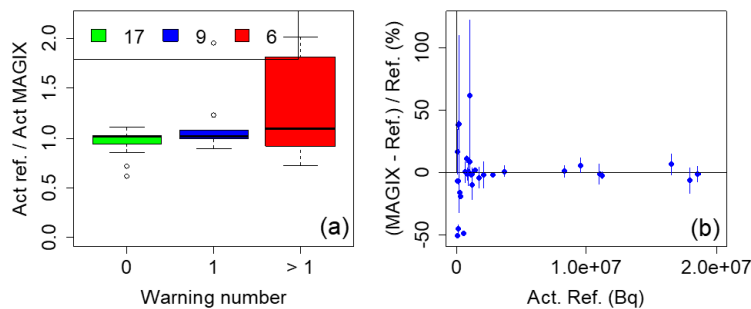


Fig. 11: Results obtained with the HPGe spectrum with the user defined efficiency: the ratios of reference activity to MAGIX activity according to the number of warnings (a) and the relative differences between MAGIX activities and the reference activities according to the reference activities (b). The numbers in the legend indicate the number of found radionuclides.

The analysis of the HPGe spectrum with the user defined efficiency and with the MAGIX detection efficiency gave close results (Fig. 11 and Fig. 12) with an interquartile range higher with MAGIX detection efficiency (0.1 with the user defined efficiency against 0.3 with MAGIX detection efficiency). The uncertainties on the activities were higher with the MAGIX detection efficiency than with the user defined efficiency because of the relative detection efficiency uncertainties (It was decided here to associate no uncertainty on the user's simulated efficiency).

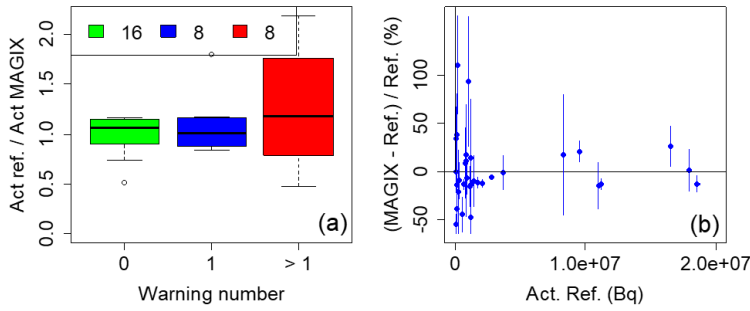


Fig. 12: Results obtained with the HPGe spectrum with the MAGIX detection efficiency: the ratios of reference activity to MAGIX activity according to the number of warnings a) and the relative differences between MAGIX activities and the reference activities according to the reference activities (b). The numbers in the legend indicate the number of found radionuclides.

3.4. Influence of energy slope

This study was performed using the HPGe spectrum with a FWHM of 0.2% at 662 keV and with the user defined efficiency. Its channels were grouped by 2, 3 and 4 in order to simulate four different energy slopes: 0.32, 0.63, 0.95 and 1.27 keV/channel. The number of radionuclides found by MAGIX decreased with the increasing energy slope, from 32 at 0.32 keV/channel to 25 at 1.27 keV/channel and whatever the number of warnings (Table 5). However, the ratios of reference activity to MAGIX activity (Fig. 13) remained close to one, whatever the slope: the median values of the ratios varied between 1.00 at 1.27 keV/channel and 1.02 at 0.63 keV/channel, with similar interquartile ranges.

Table 5: Number of radionuclides founds according to the energy slope.

	Energy slope (keV/channel)			
	0.32	0.69	0.93	1.27
0 warning	17	16	13	15
1 warning	9	8	10	6
>1 warnings	6	4	5	4
Total	32	28	28	25

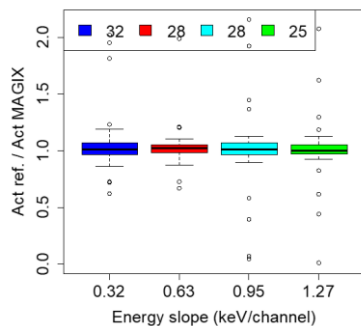


Fig. 13: The ratios of reference activity to MAGIX activity obtained with the user defined efficiency for the four energy slopes. The numbers in the legend indicate the number of found radionuclides.

3.5. Influence of resolution

This study was performed using HPGe, CZT and LaBr₃ spectra with a common slope of 0.95 keV/channel and with the user defined efficiency. The tested FWHM (at 662 keV) were 0.2% for the HPGe spectrum, 1.3% for the CZT spectrum and 3.2% for the LaBr₃ spectrum. The number of radionuclides found by MAGIX decreased strongly with resolution degradation, from 28 at 0.2% to 17 at 3.2% (Table 6). Moreover, the proportion of radionuclides found with at least two warnings increased with resolution degradation, from 17% (5/28) at 0.2% to 41% (7/17) at 3.2%. The ratios of reference activity to MAGIX activity were not so good with resolution degradation (Fig. 14): the median values of the ratio were from 1.01 at 0.2% to 1.05 at 3.2% and the interquartile ranges were from 0.1 at 0.2% to 0.5 at 3.2%.

Table 6: Number of radionuclides found according to the resolution.

	FWHM (at 662 keV)		
	0.2% (HPGe)	1.3% (CZT)	3.2% (LaBr ₃)
0 warning	13	4	5
1 warning	10	5	5
>1 warnings	5	9	7
Total	28	18	17

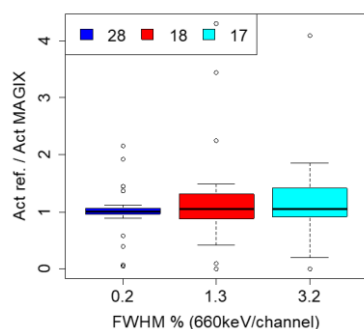


Fig. 14: The ratios of reference activity to MAGIX activity obtained with the user defined efficiency for the three resolutions. The numbers in the legend indicate the number of found radionuclides.

3.6. First use of MAGIX with measured spectra

It is difficult to evaluate the performances of MAGIX on a real setup because it requires the ability to carry out experiments on short-lived fission products. Moreover, reference activities are generally not available.

However, MAGIX is currently used to interpret gamma spectra acquired with an HPGe detector on photofission experiments where a lot of short half-life FPs are observed. Fig. 15 is an example of spectrum recorded after the photofission of a depleted uranium sample. It provides an overview of the complexity of a photofission spectrum with the signature of many fission products, in this case during 67 h after the end of irradiation by high-energy photons.

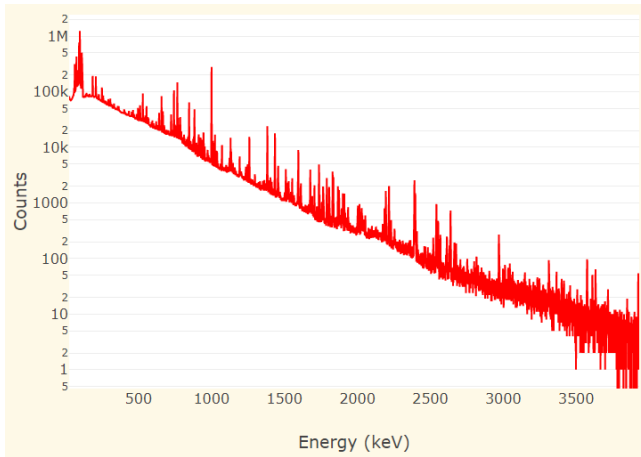
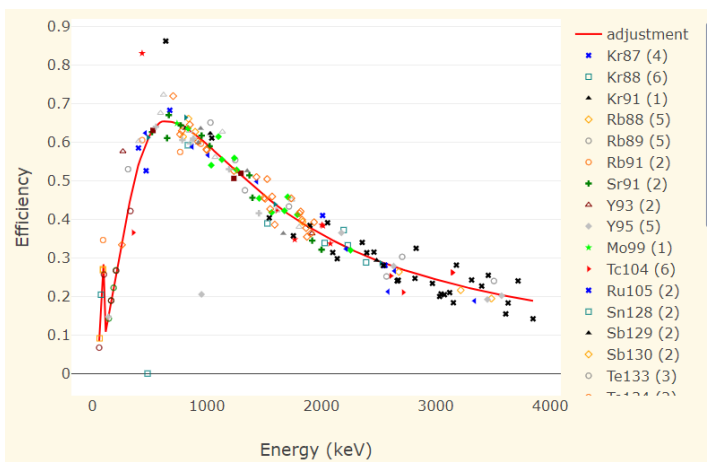
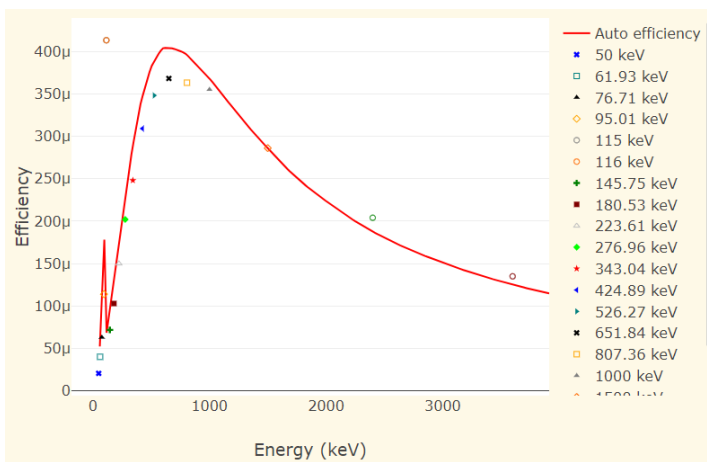


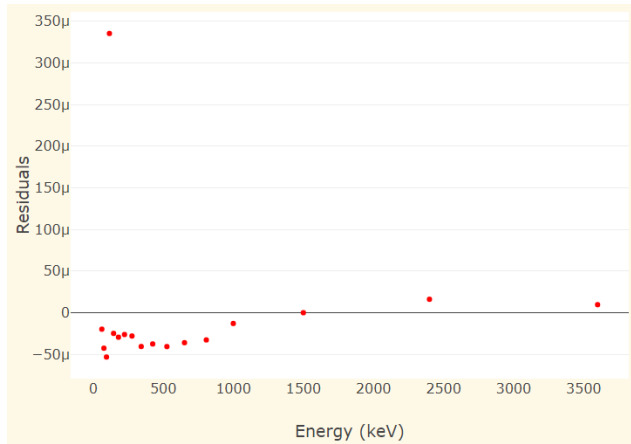
Fig. 15: Photofission spectrum of a depleted uranium sample recorded between 30 s and 67 h after the end of the irradiation by a 16 MeV Bremsstrahlung beam.



(a)



(b)



(c)

Fig. 16: (a): Relative detection efficiency curve calculated by MAGIX (red curve) after a simultaneous fitting of the model parameters of detection efficiency and mass fractions (points relative to the different peaks) (§ 2.7). (b): Detection efficiency curve calculated by MAGIX (red curve) compared to the user defined efficiency (points). (c): Residuals between user defined efficiency and MAGIX efficiency.

Radionuclide identification of such a spectrum is not convenient with a classic spectrum analysis software. Indeed, too many FPs are present to construct a database containing all the gamma ray lines attributed to the FPs. It can result in a misestimation of the net peak area of a line attributed to a wrong radionuclide in case of interference with other peaks. For example, in the case of the depleted uranium photofission, the emission of ^{234m}Pa , a natural descendent of ^{238}U , constitutes a passive background interfering with gamma rays emitted by FPs. Therefore, this may lead to an error when evaluating the radionuclide activity. This kind of problem does not occur with the MAGIX code, since it automatically filters the gamma- and X-rays database to retain only the lines considered a priori to be the most pertinent. Besides filtering a database, the MAGIX execution time for such a spectrum constitutes a major asset since it is only a couple of minutes.

In this study, the analysis was done with a known detection efficiency but Fig. 16b shows that the detection efficiency curve found by MAGIX (Fig. 16a) was very close to it. This observation reinforces the confidence in the detection efficiency curve provided by MAGIX in the case of a HPGE spectrum (§ 3.2).

The use of MAGIX allowed the identification of more than 50 FPs at the same time in the photofission delayed gamma spectrum, and the extraction of the net peak areas of several hundreds of gamma ray lines. These results enabled to calculate the cumulative photofission yields of ^{238}U for 49 FPs. As an example, data obtained with MAGIX and cumulative photofission yields published in the literature are provided in Table 7. Despite some discrepancies that are partly due to differences in the interrogating high-energy photon beam, the calculated yields are in good agreement with existing datasets, therefore enhancing the confidence in the different radionuclide activity results provided by the MAGIX code.

Table 7: Example of cumulative yields of ^{238}U photofission products calculated with MAGIX and published data (provided in number of fission products per 100 fissions).

FP	$T_{1/2}$	Yields calculated with MAGIX [14]	Carrel <i>et al.</i> data [15]	Naik <i>et al.</i> data [16]	Kahane <i>et al.</i> data [17]
^{87}Kr	1.3 h	1.96 ± 0.31	-	1.86 ± 0.30	1.82 ± 0.21
^{88}Kr	2.8 h	2.24 ± 0.34	2.52 ± 0.23	2.58 ± 0.19	-

⁹¹ Sr	9.7 h	3.86 ± 0.60	4.53 ± 0.22	3.69 ± 0.23	3.81 ± 0.45
¹⁰⁴ Tc	18.3 min	3.60 ± 0.56	-	3.65 ± 0.28	4.13 ± 0.50
¹⁰⁵ Ru	4.4 h	2.76 ± 0.44	-	2.55 ± 0.06	2.95 ± 0.45
¹⁴² Ba	10.6 min	4.38 ± 0.78	4.66 ± 0.22	4.38 ± 0.29	-
¹⁴³ Ce	1.4 days	4.39 ± 0.68	-	4.74 ± 0.14	5.38 ± 0.62

4. Conclusion

The MAGIX code is an automatic tool for the analysis of HPGe, CZT and LaBr₃ complex gamma spectra. It was developed as part of the DECA-PF project to diagnose the state of a reactor core after a severe accident but it can analyze spectra corresponding to any other case.

It carries out a complete analysis of the spectrum with the following stages: calibration, identification of present radionuclides, deconvolution of all peaks, determination of the relative detection efficiency if detection efficiency is not included in the user input data, and calculation of activity for each radionuclide (or ratio of activities if detection efficiency is unknown). One of its main features is to include, at each step, the automatic filtering of a specific gamma- and X-rays database, depending on each spectrum and each step. It also gives many indications on the result consistency.

The analysis time for a complex spectrum is less than 5 minutes and the result is not dependent on the user. The results of the analysis are very complete: for each radionuclide, the user can access all types of information such as the lines retained in the analysis, the adjustment of these lines, the coherence between the lines, warnings, to help the user to validate or not the presence of the radionuclide.

MAGIX does not solve all problems and the results may require an expert view to check, for example, the warnings in order to validate identifications. But it can be a great help in interpreting complex spectra, even for an expert. And it saves a lot of time, especially with the automatic creation and filtering of the gamma library which is a complex operation when it has to be done manually.

The study of MAGIX performances was carried out using simulated spectra corresponding to HPGe, CZT and LaBr₃ detectors. Results obtained from the analysis of the HPGe spectrum with the user defined efficiency and with the MAGIX detection efficiency were close. The various tests showed that the number of radionuclides well identified by MAGIX decreased a little with the increasing energy slopes and strongly with resolution degradation. They also showed that the accuracy of the activities was similar with increasing energy slopes but decreased with resolution degradation.

The use of MAGIX on real photofission experiments showed a simplification in spectrum interpretation and a robustness of activity calculations.

Acknowledgments

The DECA-PF project, launched end of 2013, was sponsored by the French government “Investments for the future” program through the grant ANR-11-RSNR-0003 supervised by the French National Research Agency (ANR) under the “Research in Nuclear Safety and Radioprotection” (RSNR) research initiative.

References

- [1] IAEA, “Intercomparison of gamma ray analysis software packages, IAEA-TECDOC-1011,” Vienna, 1998.
- [2] Canberra, “Genie TM 2000 Spectroscopy Software – Customization Tools,” 2003.
- [3] G. Daniel, F. Ceraudo, O. Limousin, D. Maier and A. Meuris, “Automatic and Real-Time Identification of Radionuclides in Gamma-Ray Spectra: A New Method Based on Convolutional Neural Network Trained With Synthetic Data Set,” in IEEE Transactions on Nuclear Science, vol. 67, no. 4, pp. 644-653, April 2020, doi: 10.1109/TNS.2020.2969703.
- [4] G. Ducros,, P.G. Allinei, C. Roure,, C. Rozel,, N. Blanc De Lanaute, G. Musoyan., “On-line Fission Products measurements during a PWR severe accident: the French DECA-PF project,” ANIMMA International Conference, 20-24 April 2015, Lisbon, Portugal.
- [5] Simon, A.-C.; Carrel, F.; Espagnon, I.; Lemercier, M. & Pluquet, A. (2011), “Determination of actinides isotopic composition: performances of the IGA code on Plutonium Spectra according to the experimental setup,” IEEE Transactions on Nuclear Science 58, 378-385.
- [6] Espagnon, I.; Simon, A. C.; Lamadie, F. & Mahé, C. (2011), “sIGAle, a new code for automatically determining radionuclide activities using CdZnTe spectrometry,” IEEE Transactions on Nuclear Science 58, 1159-1165.
- [7] A. J. M. Plompen et al., “The joint evaluated fission and fusion nuclear data library, JEFF-3.3,” Eur. Phys. J. A, vol. 56, no 7, p. 181, juill. 2020, doi: 10.1140/epja/s10050-020-00141-9.
- [8] S. Steenstrup, “A simple procedure for fitting a background to a certain class of measured spectra,” J. Appl. Cryst., 14: 226, 1981.
- [9] “Détermination du seuil et de la limite de détection en spectrométrie gamma” (1989). <https://inis.iaea.org/collection/NCLCollectionStore/Public/21/054/21054264.pdf?r=1>
- [10] T. Goorley et al., « Initial MCNP6 Release Overview », null, vol. 180, no 3, p. 298- 315, dec. 2012, doi: 10.13182/NT11-135.
- [11] “Germanium Detectors”. <https://www.mirion.com/products/germanium-detectors>
- [12] “GR1 Family Range | CZT based gamma-ray spectrometers”, Kromek. <https://www.kromek.com/nuclear/gr1-ctz-gamma-ray-detectors/>
- [13] “Lanthinum Bromide LaBr₃(Ce) | Products | Saint-Gobain Crystals”. <https://www.crystals.saint-gobain.com/products/standard-and-enhanced-lanthanum-bromide>
- [14] M. Delarue, E. Simon, B. Perot, P.-G. Allinei, N. Estre, E. Payan, D. Eck, D. Tisseur, I. Espagnon, J. Collot, “Measurement of cumulative photofission yields of ²³⁵U and ²³⁸U with a 16 MeV Bremsstrahlung photon beam,” Nuclear Instruments and Methods in Physics Research Section A: Accelerators, Spectrometers, Detectors and Associated Equipment. 1011 (2021) 165598.
- [15] F. Carrel, M. Agelou, M. Gmar, F. Lainé, J. Lorida, J.-L. Ma, C. Passard, B. Poumarède, “New experimental results on the cumulative yields from thermal fission of ²³⁵U and ²³⁹Pu and from photofission of ²³⁵U and ²³⁸U induced by bremsstrahlung”, IEEE Trans. Nucl. Sci., vol 58, pp 2064-2072, 2011.
- [16] H. Naik, F. Carrel, G. N. Kim, F. Lainé, A. Sari, S. Normand, A. Goswami, “Mass yield distributions of fission products from photo-fission of ²³⁸U induced by 11.5-17.3 MeV bremsstrahlung”, Eur. Phys. J A, vol. 49, 2013.
- [17] S. Kahane, A. Wolf, “Photofission of ²³⁸U with neutron-capture gamma rays”, Phys. Rev. C, vol. 32, 1985.